The immersed boundary method for two-dimensional foam with topological changes

Yongsam Kim[1,*], Yunchang Seol[1], Ming-Chih Lai[2], and Charles S. Peskin[3]

[1] *Department of Mathematics, Chung-Ang University, Dongjakgu Heukseokdong, Seoul 156-756, Korea.*
[2] *Department of Applied Mathematics, Center of Mathematical Modeling and Scientific Computing, National Chiao Tung University, 1001, Ta Hsueh Road, Hsinchu 300, Taiwan.*
[3] *Courant Institute of Mathematical Sciences, New York University, 251 Mercer Street, New York, NY 10012 USA.*

Abstract. We extend the immersed boundary (IB) method to simulate the dynamics of a 2D dry foam by including the topological changes of the bubble network. In the article [Y. Kim, M.-C. Lai, and C. S. Peskin, J. Comput. Phys. 229:5194-5207, 2010], we implemented an IB method for the foam problem in the two-dimensional case, and tested it by verifying the von Neumann relation which governs the coarsening of a two-dimensional dry foam. However, the method implemented in that article had an important limitation; we did not allow for the resolution of quadruple or higher order junctions into triple junctions. A total shrinkage of a bubble with more than four edges generates a quadruple or higher order junction. In reality, a higher order junction is unstable and resolves itself into triple junctions. We here extend the methodology previously introduced by allowing topological changes, and we illustrate the significance of such topological changes by comparing the behaviors of foams in which topological changes are allowed to those in which they are not.

AMS subject classifications: 65-04, 65M06, 76D05, 76M20

Key words: foam, permeability, capillary-driven motion, immersed boundary method, coarsening, topological changes, T1 and T2 processes

1 Introduction

We use the immersed boundary (IB) method [10] to simulate the dynamics of a 2D dry foam, including the topological changes of the foam structure. Liquid foam is a gas-filled

*Corresponding author. *Email addresses:* enviho@gmail.com (Y. Seol),mclai@math.nctu.edu.tw (M.-C. Lai), peskin@cims.nyu.edu (C.S. Peskin),kimy@cau.ac.kr (Y. Kim)

space divided into bubbles or cells of which the boundaries are liquid. In a "dry" foam, in which most of the volume is attributed to its gas phase, the bubbles are nearly polyhedral in shape. The thin liquid boundaries move under the influence of surface tension and have permeability which allows the gas to move through the thin liquid boundaries. Thus the capillarity and gas exchange between bubbles together result in the evolution in bubble size and topological structure [12]. This process is called diffusive coarsening. The diffusive flux of gas through a liquid boundary is proportional to the pressure difference between the two bubbles that are separated by that boundary.

In [5], we have applied and extended the immersed boundary (IB) method to simulate the dynamics of a dry foam in the two-dimensional case, and tested it by verifying the von Neumann relation [8,9]: let A be the area of one bubble of a foam, then

$$\frac{dA}{dt} = -M\gamma \int_\Gamma \kappa dl = -2\pi M\gamma \left(1 - \frac{n}{6}\right), \tag{1.1}$$

where M, γ, κ, and n are the permeability coefficient, surface tension, curvature of the bubble boundary Γ, and the number of vertices of the bubble, respectively. The von Neumann relation simply says that the area is constant for 6-sided bubbles, that bubbles with fewer than 6 sides tend to disappear (and in fact reach zero area in finite time), and that bubbles with more than 6 sides tend to grow; hence the "coarsening" of the foam, in which bubbles with large numbers of sides grow at the expense of bubbles with small numbers of sides.

We verified numerically the von Neumann relation in [5] and we showed there the capability of the IB method to simulate the dynamics of a foam with an arbitrarily general shape which experiences the coarsening due to the gas diffusion through the bubble boundaries. An important limitation of the numerical method used in [5], however, was that we did not allow for the resolution of quadruple or higher order junctions into triple junctions. The total disappearance of a bubble with four or more edges generates quadruple or higher order junction at which the exterior angles are no longer equal to $2\pi/6$, as was assumed in the derivation of the von Neumann relation (1.1). In reality, higher order junctions are unstable and resolve themselves into a pair of triple junctions, with the creation of a new edge that arises at zero length and grows in length as the two triple junctions move apart.

We now extend the methodology of [5] and introduce a method to resolve quadruple or higher order junctions into triple junctions. The extension is based on two primary topological changes which may occur in the evolution of a bubble network [3, 12]. The first one, which is called a T1 process, is needed when an edge of a bubble gradually shrinks and is about to make a quadruple junction. Since a quadruple junction is unstable, after some transient, this vertex decomposes to form two triple junctions, but in a different configuration. The second one, which is called a T2 process, occurs when a three-edged bubble gradually shrinks and finally disappears. Other topological changes are also possible through the combination of these two processes. For example, a four-sided bubble can disappear by a T1 process followed by a T2 process.

The rest of the paper is organized as follows. In Section 2, we describe the equations of motion of a foam. These are the typical IB equations of motion, generalized to handle a permeable boundary under surface tension. The numerical implementation is described in Section 3 which includes the methods for the topological changes and for the initialization of a foam with a general configuration. In Section 4, we present the numerical results which simulate the foams with 50 and 200 bubbles and the foam of a hexagonal structure with a minor defect. In each case, we compare the foams with topological changes and without them. Some of the results are available as online animations on the web 'http://cau.ac.kr/∼kimy'. Summary and conclusions are in Section 5.

2 Immersed boundary formulation

We summarize the equations of motion of the foam boundaries interacting with the surrounding gas which can diffuse through the foam boundaries. The equations of motion are as follows:

$$\rho(\frac{\partial \mathbf{u}}{\partial t}+\mathbf{u}\cdot\nabla\mathbf{u}) = -\nabla p+\mu\nabla^2\mathbf{u}+\mathbf{f}, \tag{2.1}$$

$$\nabla\cdot\mathbf{u} = 0, \tag{2.2}$$

$$\mathbf{f}(\mathbf{x},t) = \int \mathbf{F}(s,t)\delta(\mathbf{x}-\mathbf{X}(s,t))ds, \tag{2.3}$$

$$\begin{aligned}\frac{\partial \mathbf{X}}{\partial t}(s,t) &= \mathbf{u}(\mathbf{X}(s,t),t)+M\mathbf{F}/\left|\frac{\partial \mathbf{X}}{\partial s}\right|,\\ &= \int \mathbf{u}(\mathbf{x},t)\delta(\mathbf{x}-\mathbf{X}(s,t))d\mathbf{x}+M\mathbf{F}/\left|\frac{\partial \mathbf{X}}{\partial s}\right|,\end{aligned} \tag{2.4}$$

$$\mathbf{F}(s,t) = \frac{\partial}{\partial s}(\gamma\boldsymbol{\tau}), \tag{2.5}$$

$$\boldsymbol{\tau}(s,t) = \frac{\partial \mathbf{X}}{\partial s}/\left|\frac{\partial \mathbf{X}}{\partial s}\right|. \tag{2.6}$$

In this system, Eqs. (2.1)-(2.2) are fluid equations, Eqs. (2.5)-(2.6) are equation for the force density of the bubble boundary, and Eqs. (2.3)-(2.4) are interaction equations. We describe the notation and meaning of each of these subsystems of equations in turn.

The fluid equations (2.1)-(2.2) are the familiar Navier-Stokes equations of a viscous incompressible fluid. The constant parameters ρ and μ are the fluid density and viscosity, respectively. The unknown functions in the fluid equations are the fluid velocity $\mathbf{u}(\mathbf{x},t)$, the fluid pressure $p(\mathbf{x},t)$, and the force per unit length applied by the bubble boundary to the fluid $\mathbf{f}(\mathbf{x},t)$, where $\mathbf{x}=(x,y)$ are fixed Cartesian coordinates, and t is the time.

The force density equations of the foam boundary (2.5)-(2.6) are written in Lagrangian form. The unknown function $\mathbf{X}(s,t)$ completely describes the motion of the bubble boundary, and also its spatial configuration at any given time. For example, if we hold s fixed,

then the equation $\mathbf{x}=\mathbf{X}(s,t)$ defines the trajectory of the material point whose coordinate is s. The functions $\boldsymbol{\tau}(s,t)$ is the unit tangent vector to the bubble boundary, and the formula for $\mathbf{F}(s,t)$ is the standard one for a fiber under tension. The constant γ is the surface tension.

Finally, we come to the interaction equations (2.3) and (2.4). These both involve the two-dimensional Dirac delta function $\delta(\mathbf{x})=\delta(x)\delta(y)$, which expresses the local character of the interaction between the fluid and boundary. Eq. (2.3) expresses the relationship between the two corresponding force densities $\mathbf{f}(\mathbf{x},t)d\mathbf{x}$ and $\mathbf{F}(s,t)ds$. To see that this is the content of Eq. (2.3), integrate both sides over an arbitrary region Ω of 2D space. On the right-hand side, interchange the order of integrations, and recall that $\int_\Omega \delta(\mathbf{x}-\mathbf{X})d\mathbf{x}$ yields the value 1 if $\mathbf{X}$ is within Ω and 0 otherwise. Note that $\mathbf{f}(\mathbf{x},t)$ is singular, whereas $\mathbf{F}(s,t)$ is not, but both have finite integrals over finite regions.

Eq. (2.4) is the equation of motion of the immersed bubble boundary, in which M is the permeability constant. Setting $M=0$, Eq. (2.4) reduces to the no-slip condition that the immersed boundary moves at the local fluid velocity. The term involving M describes the normal motion of the boundary relative to the fluid. This normal slip is a consequence of the permeability of the boundary. The specific form of this term is a consequence of three assumptions: Darcy's law relating the flux of gas to the pressure difference; the jump condition for normal stress at the immersed boundary; and the fact that the force $\mathbf{F}$ associated with the surface tension is normal to the boundary (since γ is constant, see Eq. (2.5)). For a more detailed derivation of the permeability term in Eq. (2.4), see [5]. Other methods to simulate a permeable thin boundary can be found in [6, 11].

3 Numerical scheme

In this section we summarize the computational procedures used in [5] and describe new features of the present simulations. The new features concern topological changes and the manner in which we set up the initial configuration of a foam.

3.1 Computational procedure

In order to solve numerically Eqs. (2.1)-(2.6), we use a standard first-order IB method, generalized to take a permeable foam boundary into account [4, 5]. The step-by-step procedure of the numerical implementation used here and in [5] can be summarized as follows. (See [5] for greater detail.)

(1) Using the position of the internal bubble boundary, calculate the Lagrangian force density. This is done by the discritization of Eqs. (2.5) and (2.6).

(2) Distribute this tension force defined on Lagrangian grid points into the force at Eulerian spatial grid points to be applied in the Navier-Stokes equations. This is done by a discretization of Eq. (2.3).

(3) Given the Eulerian force density, we solve the descritized version of the fluid equations (2.1)-(2.2) to update the velocity and pressure fields.

(4) Update the bubble boundary points which are moved at the local fluid velocity of the updated velocity field with correction for relative slip. This is done by approximating Eq. (2.4).

At the end of each time step, we redistribute the internal boundary points of the foam to maintain reasonable resolution along the boundary. A proper resolution of the boundary is maintained by these two processes: (1) when the distance between two neighboring boundary points is larger than $h/2$ where h is the spatial meshwidth, add a new immersed boundary point halfway between them, or (2) when the distance between two neighboring boundary points is smaller than $h/4$, delete both points and create in their place a new boundary point halfway between them.

In addition to the redistribution of the internal boundary points, we now perform topological changes when they are needed at the end of each time step. This is the subject of the following section.

3.2 Topological changes

Topological changes are needed to resolve quadruple or higher order junctions into triple junctions. Since a junction of more than 4 edges is unstable, it should be resolved into triple junctions. Moreover the coarsening process cannot complete without the resolution process [5]. The topological changes of a 2D foam network can all be described in terms of two primary topological processes [3, 12]: (1) removal of an edge between two neighboring bubbles, so that they cease to be neighbors, and its replacement by an edge between two other bubbles that consequently become neighbors ('T1' process), and (2) the removal of a three-sided bubble ('T2' process). Other topological changes are also possible through the combinations of these two processes. For example, a four-sided bubble can disappear by a T1 process followed by a T2 process.

The T1 process is needed when an edge of a bubble gradually shrinks and is about to make a quadruple junction. This unstable vertex now decomposes to form two triple junctions, but in a different configuration, see Figure 1. The effect of T1 process is to reduce by one the number of edges of two bubbles, and to increase by one the number of edges of two other bubbles.

In order to realize the T1 process, we count the number of internal boundary points on each bubble edge at each iteration. We declare that the edge is a candidate for switching when and only when there are no interior points on an edge, i.e., when the two vertices of the edge are connected directly to each other, see the left plot of Figure 1. When an edge with only two vertices is candidate for switching, we try the switch but actually make it only if it lowers the total energy (i.e., total length) of the bubble boundary. The meaning of "try the switch" is to rotate the edge by 90 degrees about its center, to break the old connections, and to make the new ones by connecting the rotated edge to the other four edges which previously formed the two triple junctions, see Figure 1. Since this switch involves breaking four links and creating four new ones, it is only the lengths of these links l_i and l_i', i=1, 2, 3, 4 that we need to consider in deciding whether to make the actual

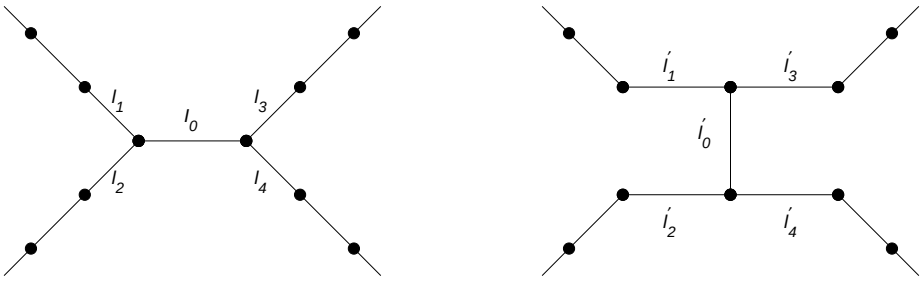

Figure 1: T1 process: a bubble edge on which there are no interior marker points is a candidate for switching (left). We rotate the edge by 90 degrees about its center, break the old connections, and make the new ones as shown (right). This switch, however, is actually made only when $\sum_{i=1}^{4} l_i \geq \sum_{i=1}^{4} l_i'$. In this case, the switch lowers the potential energy.

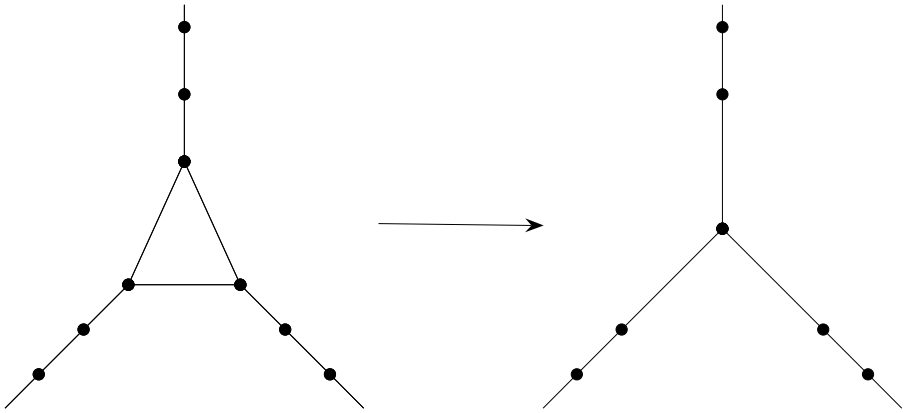

Figure 2: T2 process: whenever there are no interior points on the edges of a three-edged bubble (left), we replace the three-edged bubble by one vertex at the centroid of the bubble, and connect the new vertex directly to the three edges which previously formed triple junctions with the three-edged bubble (right).

switch or not. The actual switch is made only when it lowers the total potential energy, i.e., $\sum_{i=1}^{4} l_i \geq \sum_{i=1}^{4} l_i'$.

The T2 process is the disappearance of a 3-edged bubble when three vertices of the bubble become one point (vertex). Whenever all the edges of a 3-edged bubble have no interior points and are connected directly to each other as shown in the left plot of Figure 2, we replace the 3-edged bubble by one vertex at the centroid of the bubble, and connect the new vertex directly to the three edges which previously formed triple junctions with the 3-edged bubble, see Figure 2. As in the T1 process, since the perimeter of a disappearing triangle is always greater than the sum of the three lengths from its vertices to its centroid, the T2 process does slightly change the potential energy of the boundary, but only by lowering it. Thus, the T1 and T2 processes may be viewed as a kind of numerical dissipation of energy, and this loss of energy is part of the numerical

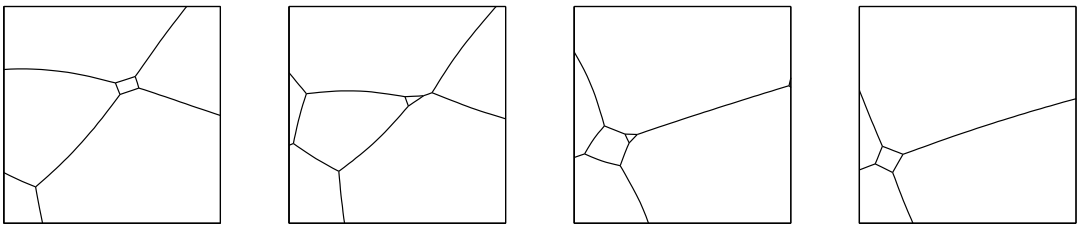

Figure 3: The effect of T1 and T2 processes. The T1 process between the 1st and the 2nd panels reduces by one the number of edges of two bubbles including the 4-edged bubble and increases by one the number of edges of two other bubbles. Then the 3-edged bubble shrinks further and disappears by the T2 process in the 4th panel.

error of the scheme.

In order to illustrate the effect of the two topological processes, Figure 3 shows the time evolution of a few bubbles, among which the initially 4-edged bubble goes through a T1 process followed by a T2 process and disappears. A T1 process occurring between the 1st and the 2nd panels changes the 4-edged bubble into a 3-edged one. It also reduces by one the number of edges of one neighboring bubble on the right side and increases by one the number of edges of two other neighboring bubbles on the upper and lower sides. Then the 3-edged bubble shrinks further in the 3rd panel and finally disappears by the T2 process in the 4th panel. Thus the 4-edged bubble disappears by the combination of T1 and T2 processes, and so can other bubbles with more than 4 edges.

3.3 Initial configurations

Consider the incompressible viscous fluid in a square $\Omega = [0,1]\times[0,1]$ with periodic boundary conditions which contains a network of bubble boundaries. We construct a Voronoi diagram to set up an initial configuration of a foam [3], see Figure 4. To do that, we first choose randomly and independently from the uniform distribution on Ω a set of points $\mathbf{Z}_1$, ..., $\mathbf{Z}_n$, where n is the desired number of bubbles. We then consider the enlarged domain $\Omega' = [-1,2]\times[-1,2]$, and make periodic images of $\mathbf{Z}_1$, ..., $\mathbf{Z}_n$ so as to obtain an enlarged list $\mathbf{Z}_1$, ..., $\mathbf{Z}_{9n}$ of points in Ω', of which the first n are the originally chosen points of Ω, and the rest are their periodic images. Now we use the built-in command 'voronoi' in Matlab to construct the Voronoi diagram with generating points $\mathbf{Z}_1$, ..., $\mathbf{Z}_{9n}$ in Ω'. This is a partition of Ω' into $9n$ convex polygons P_1, ..., P_{9n}. The defining property of the Voronoi diagram is that the interior of polygon P_k contains precisely those $\mathbf{x}\in\Omega'$ for which

$$||\mathbf{x}-\mathbf{Z}_k|| < ||\mathbf{x}-\mathbf{Z}_j|| \tag{3.1}$$

for all $j \neq k$, where $||\cdot||$ is the Euclidean norm. The restriction of the Voronoi diagram thus constructed on Ω' to Ω is then the Voronoi diagram on Ω regarded as a periodic domain. (We assume here that the maximum norm diameter of each of the P_k is less than the period of the domain, which will be true with high probability when n is reasonably large.)

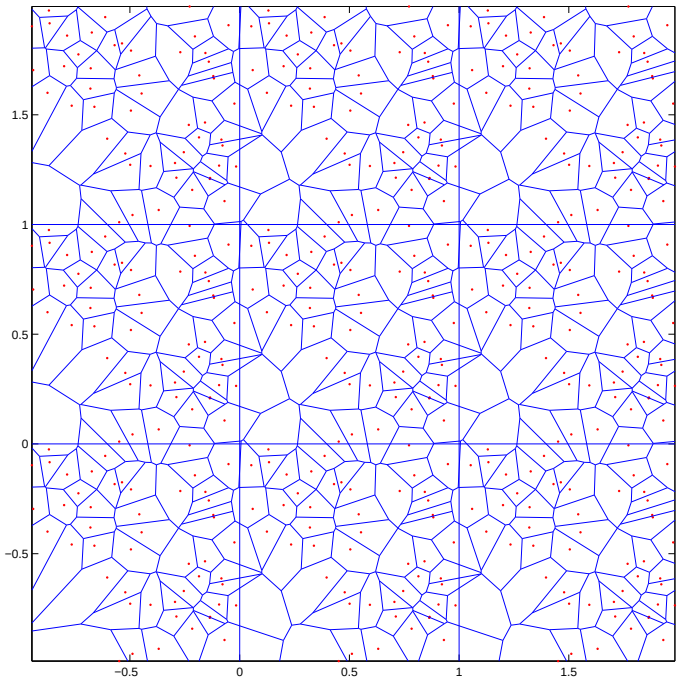

Figure 4: A set of points (50 dots) is randomly chosen in a square $[0,1]\times[0,1]$ and copied periodically into $[-1,2]\times[-1,2]$. A Voronoi network is then constructed on the enlarged domain. The restriction of this network to the domain $[0,1]\times[0,1]$ is the periodic Voronoi network generated by the original 50 points

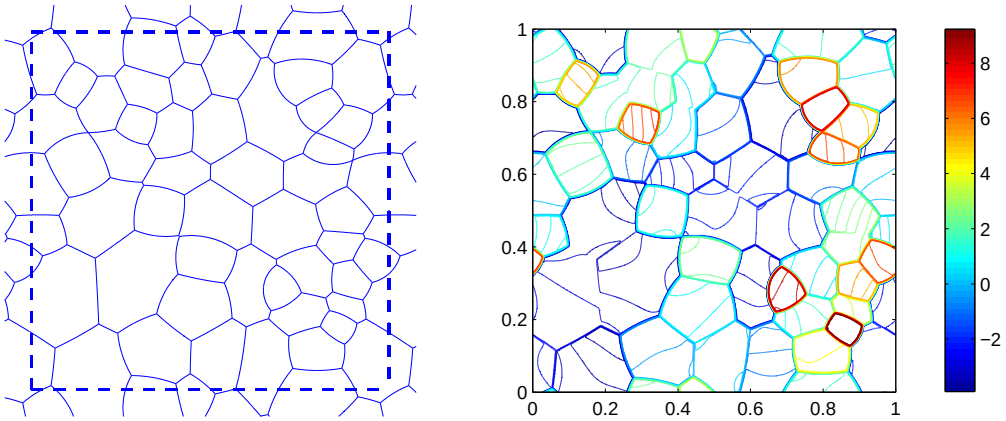

Figure 5: Initial configuration: the 'relaxed' configuration of a foam (left) obtained from the Voronoi network shown in Figure 4 and the corresponding pressure contours (right). The dashed line in the left panel represents the periodic unit square. Note that bubble boundaries are not explicitly drawn in the right panel. They are visible anyway because the steep pressure gradient across the bubble boundaries makes the pressure contours concentrate along those boundaries.

Since the Voronoi network as an initial configuration of a foam is composed of a set of straight lines, we relax the initial bubble network to obtain a more realistic shape of a foam in which the bubbles are curved polygons and all the exterior angles at the triple junctions are close to $2\pi/6$. To do that, we allow the given Voronoi network to evolve according to the methods of the present paper but with zero permeability, so that the bubbles change shape without changing area. This initial relaxation phase of the computation is continued until the pressure changes with respect to time are small, which signifies that the foam has reached a near-equilibrium state in the absence of permeability. This relaxed state is then used as an initial condition for a computation with nonzero permeability.

Figure 5 shows a 'relaxed' configuration of the foam (left) obtained from the Voronoi network shown in Figure 4 and the corresponding pressure level contours (right). The dashed line in the left figure represents the periodic unit square. Note that the pressure contours enable us to recognize the configuration of the foam without even drawing the internal foam boundaries. The bold colors in the pressure contours are mainly near the internal foam boundaries indicating that the largest pressure differences are across these internal boundaries.

4 Results and Discussion

In this section, we show the simulation results obtained by the numerical scheme presented in Section 3. The foams have general configurations and go through topology changes based on the T1 and T2 processes. Some of the results are also available as online animations, see 'http://cau.ac.kr/∼kimy'.

Throughout this paper, we choose the computational domain $\Omega = [0,1]\times[0,1]$ with periodic boundary conditions, and use the mesh width $h=\Delta x=\Delta y=1/512$, which is uniform and fixed in time, and the time step duration $\Delta t = 1.25\times10^{-6}$. The fluid density is chosen as $\rho=1$, the viscosity $\mu=0.001$, and the surface tension coefficient $\gamma=1$. Note that these parameters are arbitrarily chosen and do not correspond to any particular physical case. We use the permeability M=0.04 to see how the permeability affects the foam dynamics.

As the first case, we start with the foam shown in Figure 5 which has 50 bubbles and compare two cases: one in which the topological changes are allowed to occur, and the other in which they are not. Figure 6 shows the motion of the foams without topological changes (upper panels) and with topological changes (lower panels) at some selected times: $t=0.3$ (left), $t=0.6$ (middle), and $t=0.9$ (right). In both cases, whereas the bubbles with fewer than 6 edges shrink and disappear, the bubbles with more than 6 edges are growing in area as time goes on. Thus the overall result of these changes in area is the diffusive coarsening of the foam structure.

When there is no topological changes, as in the upper panels, however, the bubbles with fewer than 6 edges shrink, almost disappear, and form quadruple or higher order

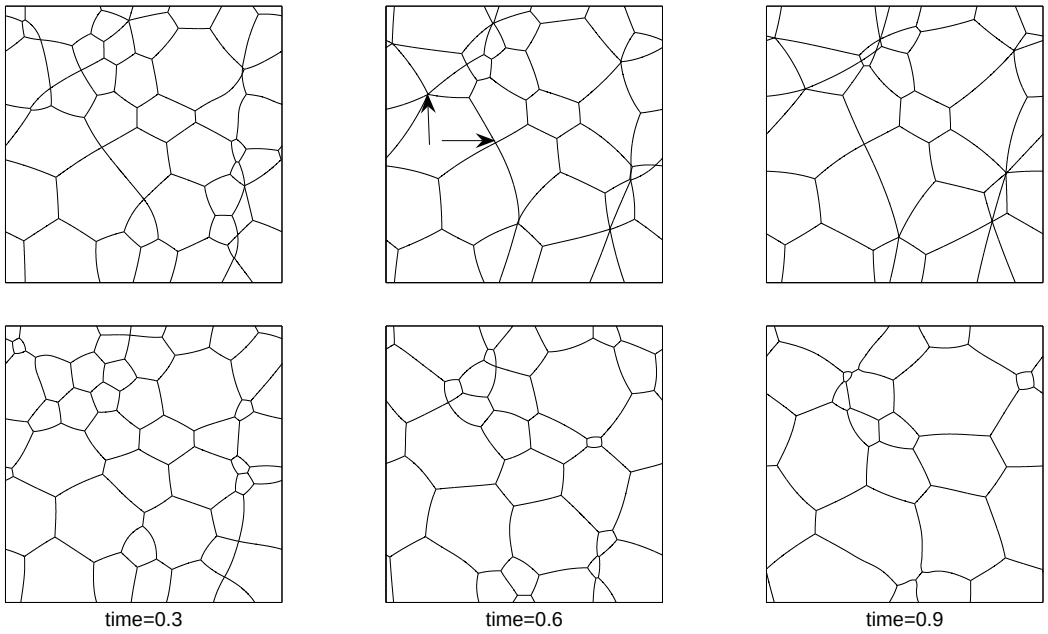

Figure 6: The motion of the foams without topological changes (upper panels) and with topological changes (lower panels) at some selected times: $t=0.3$ (left), $t=0.6$ (middle), and $t=0.9$ (right). In both cases, we can observe the diffusive coarsening of the foam structure. Whereas the foam without topological changes generates some higher order junctions, however, the foam with topological changes resolves higher order junctions into triple junctions.

junctions. See for example the two arrows in the upper-middle panel in which two bubbles with four and five edges shrink to make two higher order junctions. When a higher order junction forms in the course of our simulations, since it remains as such without any topological changes, it is in fact made up of the bubble which almost disappears and thus has a negligible area. As time proceeds, triple or higher order junctions can meet to form a junction with even higher order, see the upper-right panel. The foam with topological changes resolves higher order junctions into triple ones in the lower panels, in which case the foam moves in a more realistic way.

In order to see in a more quantitative way the difference between the two cases, we compare the number of bubbles as a function of time. The upper panels in Figure 7 show the distribution of the number of bubbles (y-axis) which have any given number of edges (x-axis). The initial distributions are the same for the two cases with and without topological changes as shown in the graph at time 0. Although the distribution is constant without topological changes and remains the same as the one at time 0, it changes over time with topological changes. The lower panel compares the total number of bubbles of the foams without (dotted line) and with (solid line) topological changes as functions of time. Again, the total number of bubbles is constant at 50 without topological changes, but it decreases over time from 50 to 17 with topological changes, which clearly indicates the diffusive coarsening process of the foam. A similar statistical behavior of the foam

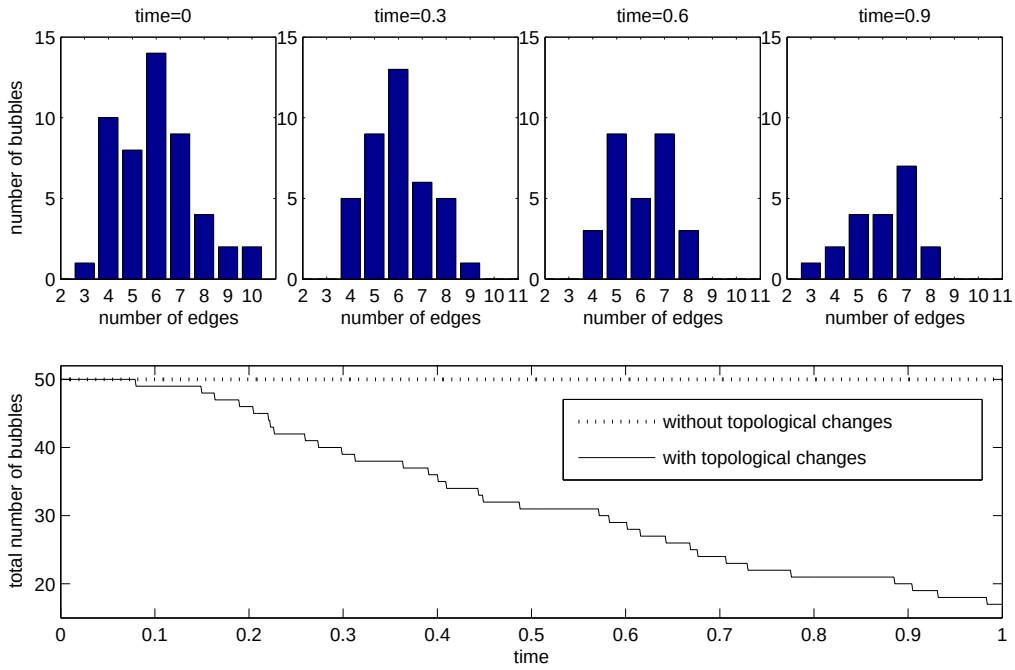

Figure 7: The distributions of the numbers of bubbles which have any given number of edges for the foam with topological changes (upper panels), and the total number of bubbles of the foams as a function of time (lower panel) for foams without (dotted line) and with (solid line) topological changes. While the distribution and total number of bubbles are constant in time without topological changes, they vary over time in a decreasing manner with topological changes. Note that the upper left panel corresponding to the initial time is applicable to both simulations, with and without topological changes. The subsequent upper panels pertain only to the case in which topological changes occur, since the edge-number distribution obviously remains constant if there are no topological changes.

structure can be found in [1, 3, 13, 14].

Figure 8 compares the areas of three chosen bubbles as functions of time for the two cases: the foams without (dotted line) and with (solid line) topological changes. The three bubbles initially have 6, 7, and 8 edges, respectively. While these numbers of edges are constant without topological changes, they vary in time with topological changes, see the numbers on the solid line in each panel. The von Neumann relation (1.1) says that the area of an inner bubble changes linearly as a function of time, increasing for bubbles with more than 6 edges, and decreasing for bubbles with fewer than 6 edges. We can see clearly that the bubble areas of the foam without topological changes do not follow the von Neumann relation, simply because the slopes of the areas plotted as functions of time are not constant, see the dotted lines.

In order to check the von Neumann relation quantitatively for the foam with topological changes, since the number of edges of the chosen bubbles may change, we should also change the edge number n in Eq. (1.1). The dashed lines in the figure represent the von Neumann relation with the properly chosen number of edges n. The bubble areas

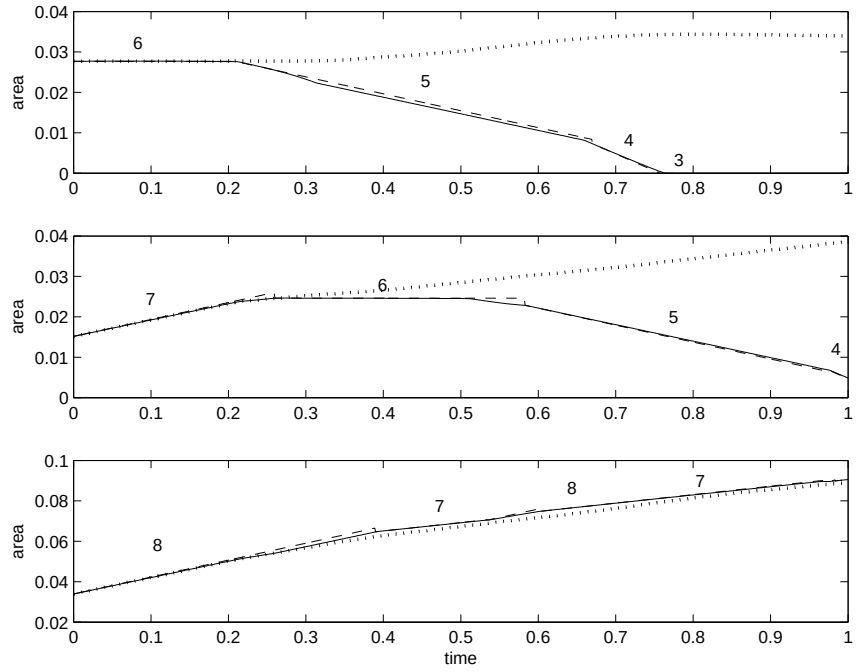

Figure 8: The areas of three selected bubbles as functions of time for the two cases: foams without (dotted line) and with (solid line) topological changes. The numbers on the solid lines represent the number of edges of each bubble, which vary in time only with topological changes. The dashed lines represent the von Neumann relation (1.1) with the corresponding number of edges n. Note that the agreement with the von Neumann relation is almost perfect when topological changes are allowed to occur. Without topological changes, the von Neumann relation is violated, as expected, once higher order junctions form.

represented by solid lines are almost linear as functions of time for each fixed number of edges and follow closely the von Neumann relation. Notice, however, that there exist appreciable deviations of the area changes from the theory near the singular points of the graphs. These singular points represent the moment of topological changes, especially T1 process. We attribute these deviations to the following: when a T1 process is about to occur, one of the bubble edges almost shrinks and the foam generates a transient quadruple junction at which the exterior angles are no longer equal to $2\pi/6$, which violates the assumption of the von Neumann relation. After the T1 process, all the junctions are again triple, and the area changes of the bubbles follow again the von Neumann relation.

If all the bubbles of a foam have a hexagonal shape, since they have 6 edges, the foam does not experience topological changes and approaches quickly a state of equilibrium in which all the exterior angles at the triple junctions are $2\pi/6$. If, however, a foam with a primarily hexagonal structure contains a few bubbles with numbers of edges unequal to 6, then diffusive coarsening is initiated at these defects and spreads throughout the foam [12]. Figure 9 compares the motion of a foam with some initial defects for two cases: foams without (upper panels) and with (lower panels) topological changes. Here the defect is set up by first choosing an hexagonal bubble network and then by modifying

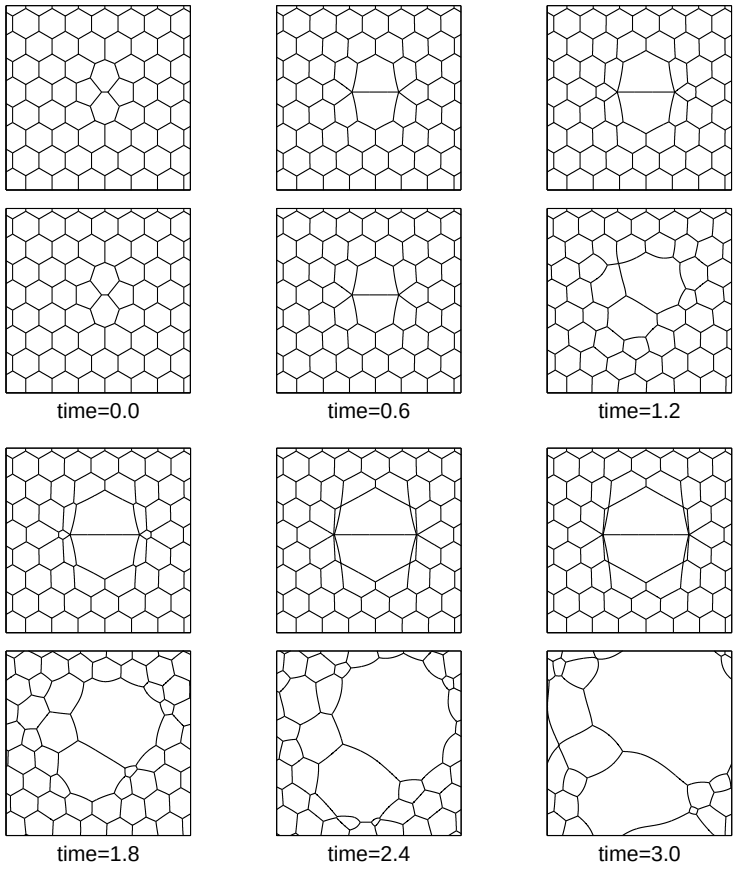

Figure 9: The spreading of a defect in a hexagonal bubble network due to the diffusive coarsening for the two cases: foams without (upper panel of each pair) and with (lower panel of each pair) topological changes. Note that the panels are arranged in pairs for easier comparison, with the two members of each pair corresponding to the same time.

it so that the central part of the foam contains two 5-edged bubbles and two 7-edged bubbles, see the first panel in Figure 9.

In the case without topological changes, the two 7-edged bubbles grow at the expense of the neighboring 5-edged bubbles. When the 5-edged bubbles disappear around time 0.6, two 5-fold junctions are generated. Then the 7-edged bubbles grow further preying on the neighboring 6-edged bubbles with a new creation of 7-fold junctions, see the picture at time 2.4. In the case with topological changes, the motion is the same as that without topological changes at early times. However, when the two 5-edged bubbles disappear around time 0.6, the foam goes through topological changes. The foam evolves further to show the diffusive coarsening process together with more topological changes. The spreading of the defect occurs in a realistic fashion only when topological changes are allowed, as shown in Figure 9 which is comparable to Figure 7.8 in [12], which was obtained by using a different numerical scheme.

Finally we simulate the coarsening process of a foam with 200 bubbles immersed in the domain $\Omega = [0,1] \times [0,1]$. Since the computational time of our method is mostly consumed in solving the fluid equations, the total computational cost is dependent only slightly on the number of bubbles. Figure 10 shows the motion of the foam with topological changes at some selected times. Whereas the foam goes through rapid topological changes and the total number of bubbles decreases rapidly at early times (upper panels), the topological changes slow down at later times (lower panels), see also the lower panel of Figure 11.

The upper panels in Figure 11 show the distribution of the number of bubbles (y-axis) which have any given number of edges (x-axis) at some selected times, and the lower panel shows the total number of bubbles of the foam as a function of time. The distribution of the bubbles varies, and the total number of bubbles decreases over time from 200 to 28, which indicates the diffusive coarsening process of the bubble network. These statistical behaviors of the foam structure have been investigated in [1, 3, 13, 14], which contain qualitatively similar figures to Figures 10 and 11.

5 Summary and Conclusions

We have used an immersed boundary method to simulate the fluid dynamics of a two-dimensional dry foam and extended the model to allow for topological changes of the bubble network. These topological changes are based on T1 and T2 processes and enable a foam to complete its total coarsening. We have compared the foam dynamics without and with topological changes. Without topological changes, there occur unrealistic quadruple or higher order junctions at which the exterior angles are no longer equal to $2\pi/6$, as was assumed in the derivation of the von Neumann relation. The topological changes as used here resolve these higher-order junctions into triple junctions and enable us to investigate the foam dynamics in a more realistic way.

A particular feature of the methodology used here is that we simulate the full fluid dynamics of the foam. Thus we do *not* make any assumption that the pressure within each bubble is uniform, or that the internal boundaries are circular arcs. This enables us to investigate foams that are far from equilibrium as easily as those that progress slowly through a sequence of near-equilibrium states.

In future work, we plan to extend the methodology introduced here to the study of three-dimensional foams [2,7]. That is, we plan to simulate the fluid dynamics of a three-dimensional dry foam by modeling the gas phase of the foam as a viscous incompressible fluid, and the liquid phase as a massless network of permeable internal boundaries under surface tension. The gas diffusion through the liquid phase of the foam can be modeled, as in the two-dimensional case, by allowing the internal boundaries to slip relative to the fluid, at a velocity (speed *and* direction) proportional to the boundary force. In 3D, the bubble boundaries can be represented as surfaces which we can model by triangulation, and the discrete force density has to be evaluated at the vertices of the triangles. The

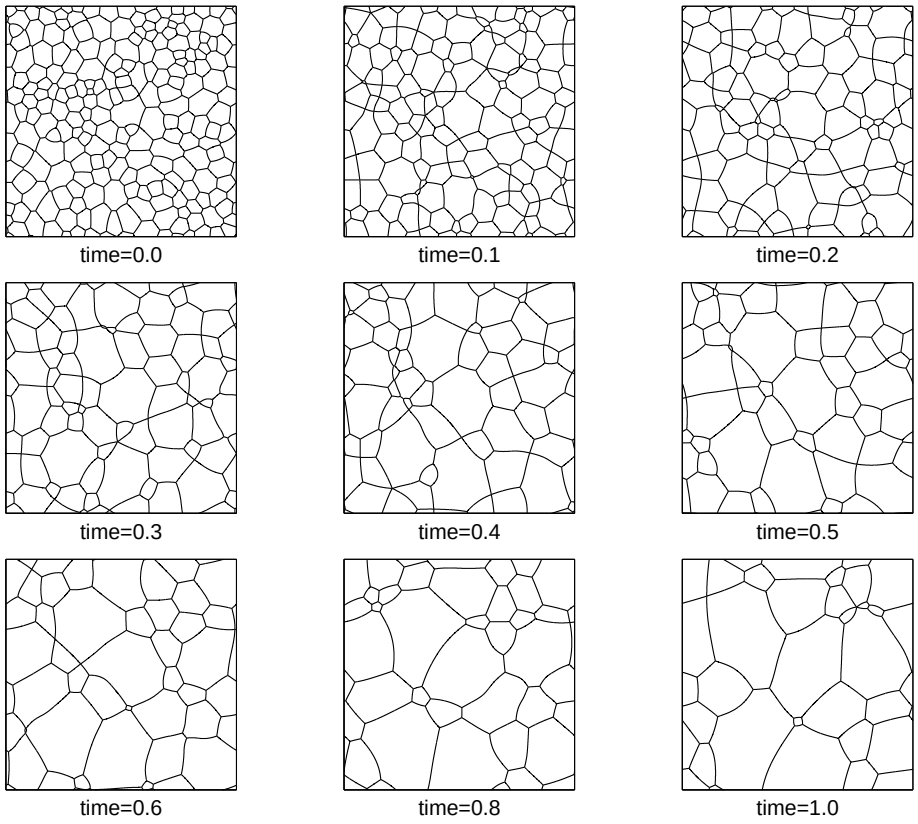

Figure 10: Diffusive coarsening of a foam which initially contains 200 bubbles, with topological changes allowed

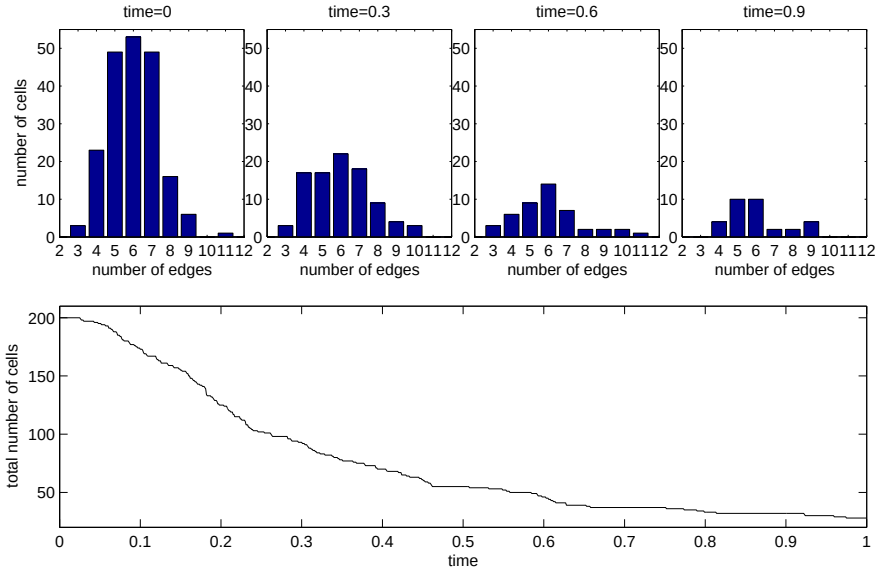

Figure 11: Results from the simulation shown in Figure 10. Upper panels show the numbers of bubbles with different numbers of edges at selected times, and the lower panel shows the total number of bubbles as a function of time.

greatest challenge of the 3D case will be the inclusion of topological changes, as in the present paper, since the types of changes that need to be considered are surely more various in 3D than in 2D.

Acknowledgement The first author was supported by National Research Foundation of Korea Grant funded by the Korean Government (2010-0016611). The second author was supported by the Chung-Ang University Research Scholarship Grant in 2010. The third author is supported in part by National Science Council of Taiwan under research grant NSC-97-2628-M-009-007-MY3, NSC-98-2115-M-009-014-MY3, and the support of NCTS in Taiwan.

References

[1] J.A. Glazier, S.P. Gross, and J. Stavans, *Dynamics of two-dimensional soap froths.* Phys. Rev. A, 36(1), 1987.

[2] S. Hilgenfeldt, A.M. Kraynik, S.A. Koehler, and H.A. Stone, *An accurate von Neumann's law for three-dimensional foams*, Phys. Rev. Lett. 86(12):2685-2688, 2001.

[3] J.P. Kermode and D. Weaire, *2D-Froth: a program for the investigation of 2-dimensional froths.* Computer Physics Communications 60, 75-109, 1990.

[4] Y. Kim and C.S. Peskin. *2-D parachute simulation by the Immersed Boundary Method.* SIAM J.Sci.Comput. 28(6), 2006.

[5] Y. Kim, M.-C. Lai, and C.S. Peskin, *Numerical simulations of two-dimensional foam by the immersed boundary method.* J. Comput. Phys. 229:5194-5207, 2010.

[6] A.T. Layton, *Modeling water transport across elastic boundaries using an explicit jump method.* SIAM J. Sci. Comput. 28(6):2189-2207, 2006.

[7] R.D. MacPherson and D.J. Srolovitz, *The von Neumann relation generalized to coarsening of three-dimensional microstructures,* Nature, 446(26):1053-1055, 2007.

[8] W.W. Mullins, *in Metal Surfaces: Structure, Energetics, and Kinetics.* (eds. W.D.Robertson and N.A.Gjostein) 17-66(American Society for Metals, Metals Park, Ohio, 1963).

[9] von Neumann, J. in Metal Interfaces (ed. C.Herring) 108-110(American Society for Metals, Cleveland, 1951).

[10] C.S.Peskin, *The immersed boundary method.* Acta Numerica, 11:479-517, 2002.

[11] J.M. Stokie, *Modelling and simulation of porous immersed boundaries.* Computers Structures 87(11-12): 701-709, 2009.

[12] D. Weaire and S. Hutzler, *The Physics of Foams*. Oxford University Press, 1999.

[13] D. Weaire and J.P. Kermode, *Computer simulation of a two-dimensional soap froth I. Method and motivation.* Phil. Mag. B. 48(3), 245-259, 1983.

[14] D. Weaire and J.P. Kermode, *Computer simulation of a two-dimensional soap froth II. Analysis of results.* Phil. Mag. B. 50(3), 379-395, 1984.